

Optical Gating of Black Phosphorus for Terahertz Detection

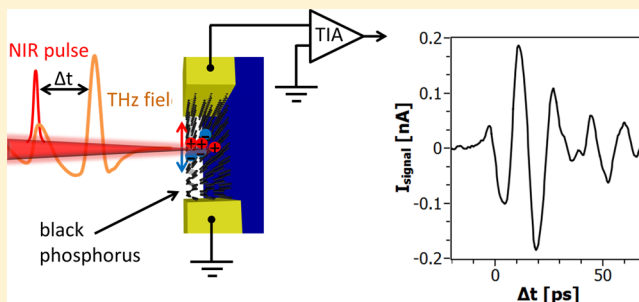
Martin Mittendorff,^{*,†,‡} Ryan J. Suess,^{†,‡} Edward Leong,[‡] and Thomas E. Murphy^{†,‡}

[†]Institute for Research in Electronics and Applied Physics, University of Maryland, College Park, Maryland 20740, United States

[‡]Department of Electrical and Computer Engineering, University of Maryland, College Park, Maryland 20740, United States

ABSTRACT: Photoconductive antennas are widely used for time-resolved detection of terahertz (THz) pulses. In contrast to photothermoelectric or bolometric THz detection, the coherent detection allows direct measurement of the electric field transient of a THz pulse, which contains both spectral and phase information. In this Letter, we demonstrate for the first time photoconductive detection of free-space propagating THz radiation with thin flakes of a van der Waals material. Mechanically exfoliated flakes of black phosphorus are combined with an antenna that concentrates the THz fields to the small flake ($\sim 10 \mu\text{m}$). Similar performance is reached at gating wavelengths of 800 and 1550 nm, which suggests that the narrow bandgap of black phosphorus could allow operation at wavelengths as long as $4 \mu\text{m}$. The detected spectrum peaks at 60 GHz, where the signal-to-noise ratio is of the order of 40 dB, and the detectable signal extends to 0.2 THz. The measured signal strongly depends on the polarization of the THz field and the gating pulse, which is explained by the role of the antenna and the anisotropy of the black phosphorus flake, respectively. We analyze the limitations of the device and show potential improvements that could significantly increase the efficiency and bandwidth.

KEYWORDS: 2D materials, black phosphorus, THz detection, photoconductivity



Photoconductive terahertz (THz) antennas made of GaAs are commonly used for time-resolved detection of THz pulses at a gate wavelength of 800 nm.^{1–4} An ultrashort laser pulse at a wavelength of about 800 nm excites electron–hole pairs in the semiconductor material and the THz field accelerates the generated carriers producing a current that is measured as a function of the time delay between THz and gate pulse. In contrast to power sensitive detectors like bolometers or photothermoelectric detectors, this technique enables a direct sampling of the electric field transient of a THz pulse. From this transient, the spectral content and phase information can be extracted via Fourier transform. In the recent years, significant effort has been devoted to developing photoconductive THz antennas that work at longer wavelengths, especially in the telecom band around $1.55 \mu\text{m}$.^{5–7} To achieve a low bandgap in combination with high carrier mobility and low conductivity, complex heterostructures are fabricated by molecular-beam epitaxy.^{8,9} Such heterostructures even allow the fabrication of large area THz photoconductive emitters^{10,11} and detectors¹² for $1.55 \mu\text{m}$ excitation. A new narrow bandgap material that has gained interest is black phosphorus. Similar to graphene, it can be mechanically exfoliated to thin flakes¹³ that can be transferred to any substrate. The high mobility in this material in combination with the low bandgap of about 0.3 eV^{14,15} makes this material interesting for optoelectronic applications at wavelengths out to $4 \mu\text{m}$.¹⁶ Detection of sub-bandgap THz radiation has been demonstrated using with antenna coupled flakes of black phosphorus, based on rectification in field-effect transistors, bolometric, and photo-

thermoelectric effects.^{17–20} Here, we present a photoconductive antenna based on exfoliated multilayer black phosphorus. Our device uses a log-periodic antenna with a multilayer flake of black phosphorus in its center. We demonstrate optically gated THz detection at gating wavelengths of 800 nm and $1.55 \mu\text{m}$. The maximum spectral sensitivity is reached at a frequency of 60 GHz with a signal-to-noise ratio above 100, for higher frequencies the detection sensitivity drops of and reaches the noise level at several hundred GHz.

The device was fabricated by mechanical exfoliation from a bulk black phosphorus crystal and subsequent photolithography. The contacts to the black phosphorus flake define a self-complementary log-periodic antenna that concentrates the THz field to the micrometer sized flake. The tooth angle as well as the bow angle is 45° , the maximum radius $r_1 = 500 \mu\text{m}$, and the radii of the shorter teeth is calculated via $r_{n+1} = 0.8r_n$ (cf. sketch in upper right corner of Figure 1). As thin flakes of black phosphorus are not stable in ambient air, the device is capped by a 100 nm thick layer of Al_2O_3 that is deposited via atomic-layer deposition.²¹ With this capping layer, the devices are stable for several months and do not show any signs of degradation. Gating measurements are carried out to estimate the mobility in our devices and reveal a mobility of about $900 \text{ cm}^2/(\text{Vs})$. Further details about the device fabrication can be found in the refs 16 and 20.

Received: July 10, 2017

Revised: August 16, 2017

Published: August 18, 2017

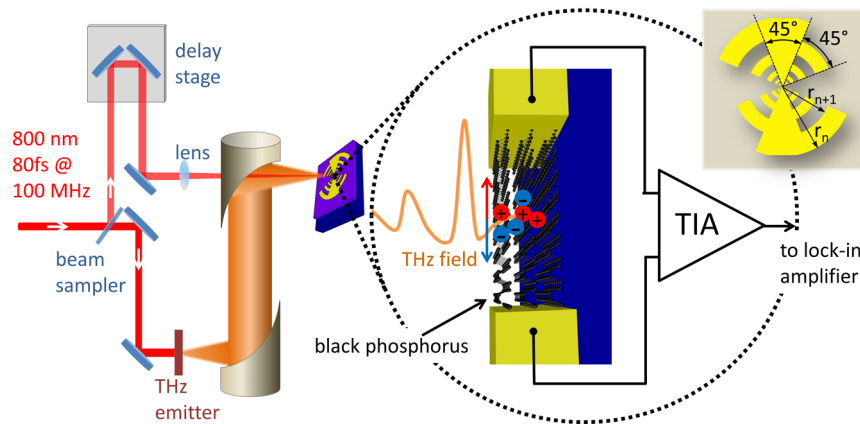


Figure 1. Diagram of the THz time-domain spectroscopy setup. A GaAs-based THz emitter is pumped by a short pulsed laser, the THz beam is collimated and refocused by a pair of off-axis parabolic mirrors. The right part of the figure shows the working principle of the THz detection; the sketch in the upper right corner shows the design of the antenna.

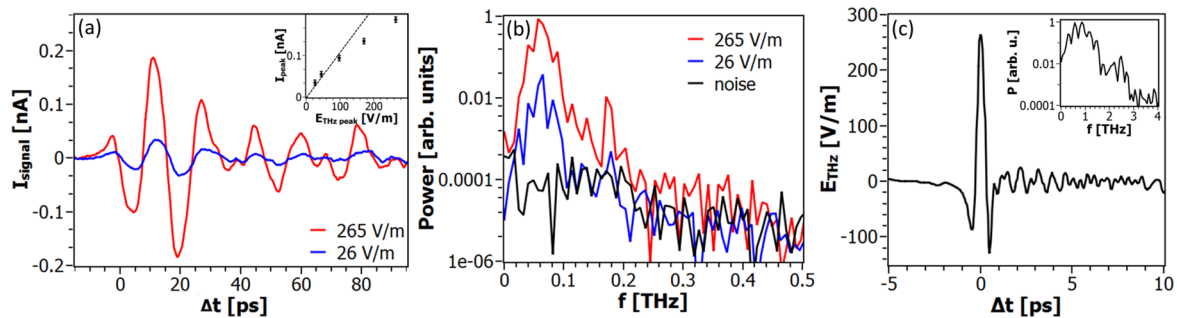


Figure 2. (a) THz transient measured at two different THz peak fields. (b) THz spectra calculated via Fourier transform from the measurements in (a). (c) Incident THz waveform measured with a ZnTe crystal via electro-optic sampling.

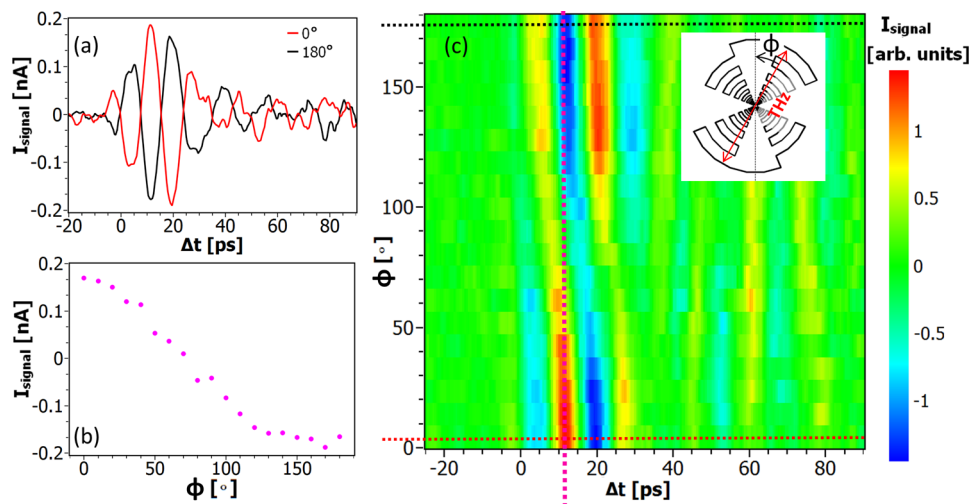


Figure 3. (a) THz transient measured at opposite THz polarization. (b) Peak current as a function of the polarization angle. (c) The measured current is color coded as a function of the time delay between the gating and the THz pulse and the polarization of the THz pulse.

The device is tested in a standard time-domain spectroscopy setup that is driven by a femtosecond laser at 800 nm. A large-area photoconductive THz emitter based on GaAs served as broadband THz source.²² Off-axis parabolic mirrors are used to collimate and refocus the THz radiation onto the detector. A small amount of the 800 nm radiation (10 mW) is split off with a beam sampler and serves as gate pulse with a fluence of 125 $\mu\text{J}/\text{cm}^2$ for the photoconductive THz detection. The gate pulse passes a variable delay stage that is used to vary the time delay

between the THz pulse and the gate pulse at the detector position. A sketch of the experimental setup and the device is shown in Figure 1. The near-infrared gate pulse generates electron–hole pairs in the black phosphorus flake; the THz field accelerates the carriers which produces a current through the transimpedance amplifier (TIA) that is connected to the device. The polarity of the emitted THz field was periodically modulated by applying a 2.5 kHz sinusoidal bias voltage to the emitter, and the photoconductive current was then synchro-

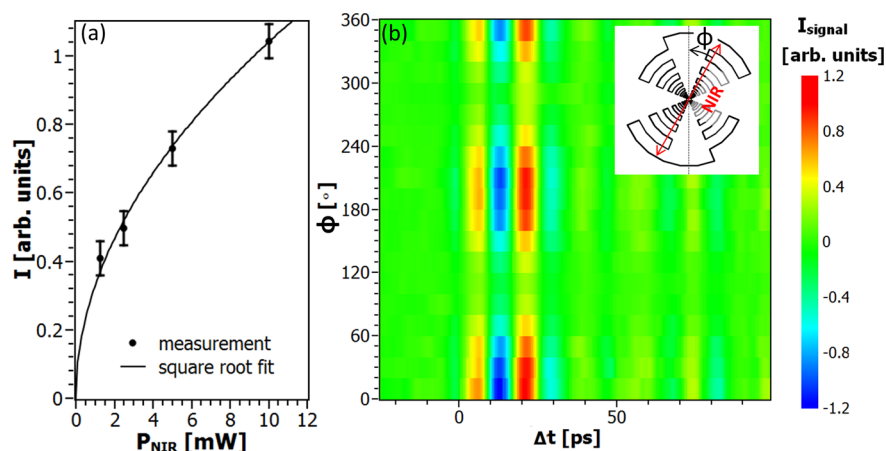


Figure 4. Peak current as a function of the applied NIR power. The dots represent the measured values; the line corresponds to a square root fit. The measured current is color coded as a function of the time delay between the gating and the THz pulse and the polarization of the NIR pulse.

nously measured via lock-in detection. To estimate the peak THz field incident on the receiver, we replaced the photoconductive detector with a 0.5 mm thick $\langle 110 \rangle$ -oriented ZnTe crystal, which has a known electrooptic coefficient. A peak, on-axis field of about 250 V/m was measured at the focal plane when the emitter was pumped with a pulse energy of 3.75 nJ at 80 MHz repetition rate.

A second setup based on two synchronized fiber lasers was used to test the THz detection at a gating wavelength of 1.55 μm . To scan the time delay between THz and gating pulse, the repetition rate of the two lasers was slightly detuned.²³ One of the fiber lasers was frequency doubled for the THz pulse generation at 780 nm using the same GaAs photoconductive THz emitter described previously.

Figure 2a shows the photocurrent as a function of the time delay for THz peak fields of 265 and 26 V/m. At the highest THz field, a signal-to-noise ratio (SNR) of 40 dB is achieved. The measured current scales slightly sublinear to the applied THz field (cf. Figure 2a), which is varied via the bias voltage of the photoconductive emitter. From the measured THz transients, the spectrum is found via the Fourier transformation (cf. Figure 2b). The spectrum exhibits a peak near 60 GHz and falls with frequency, reaching the noise level at around 0.2 THz. The incident THz waveform (and associated spectrum), measured by electro-optic sampling in a 500 μm thick ZnTe crystal is shown for comparison in Figure 2c.

To characterize the polarization dependence of the detector, the photoconductive emitter, and therewith the polarization of the THz field, was rotated by 180° with a rotational stage. Figure 3a shows the measured current as a function of the time delay between gating and THz pulse at 0° and 180° THz polarization angle. As the electric field of the THz pulse is inverted, also the measured current changes its sign. The measured peak current as a function of the polarization angle is shown in Figure 3b. The measured current is shown in the color coded plot in Figure 3c as a function of the time delay (x -axis) and the polarization angle (y -axis). When the current reaches its maximum (at 0° and 180°), the THz field is oriented along the high mobility axis of the black phosphorus flake, which is aligned to the contacts within about 20° (cf. Figure 2b in ref 20). At these orientations, however, the antenna functions like a bow-tie antenna which has maximum coupling at 0° and 180°.

The influence of the gating beam polarization and power on the THz detection is investigated next. In former studies with similar devices that are excited with femtosecond laser pulses, the photoconductivity of black phosphorus photodetectors scales with the square root of the applied power.¹⁶ This square-root scaling was attributed to radiative recombination that scales with the square of the photoexcited carriers. Pump-probe studies also show a faster carrier relaxation for higher excitation densities:²⁴ at a low pump fluence of 3 $\mu\text{J}/\text{cm}^2$, the carrier relaxation is characterized by a single-exponential decay with a time constant of 770 ps. At an increased fluence of 80 $\mu\text{J}/\text{cm}^2$, a fast component with a relaxation time of 180 ps dominates the carrier relaxation. While the peak change in current scales linearly with the number of photoexcited carriers, the faster recombination time leads to a sublinear increase of the average current.¹⁶ Similar to that, the measured average photocurrent induced by the THz field can be described by a square root fit (cf. Figure 4a). For conventional photoconductive switches, a similar saturation behavior is reported (for example, ref 25). In those cases, the saturation effect is attributed to a screening effect by the photoexcited carriers. As the carrier density in black phosphorus is only slightly changed by the gating pulse (below 1% at the power applied in our experiments), we can exclude screening as major contribution to the saturation. In Figure 4b, the measured current is plotted versus the time delay between THz and gating pulse and the NIR polarization. In contrast to the dependence on the THz polarization, where a change in sign was observed when the polarization is rotated by 180°, the sign of the signal stays constant and we observe a pronounced polarization dependence of the measured current amplitude. This dependence is not caused by the antenna, but the corrugated crystal structure of black phosphorus: similar to graphite, black phosphorus consists of layers of hexagonally arranged atoms, but unlike graphene the single sheets are not flat (cf. sketch in Figure 1). Along the zigzag direction, the mobility and optical absorption are minimized, while the maximum mobility and optical absorption are observed for electric fields in armchair direction.^{14,26} This anisotropy of optical properties has also been reported in photocurrent measurements²⁷ that show a maximized signal when the polarization is oriented perpendicular to the corrugations in black phosphorus. Hence, we can use the maximum of our signal to estimate that the high mobility

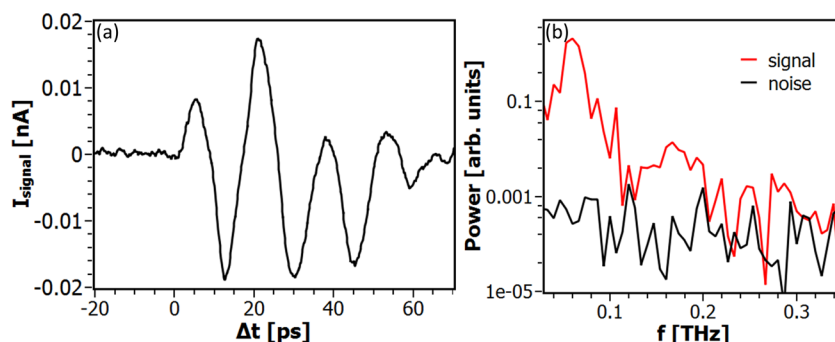


Figure 5. (a) THz transient measured at a probe wavelength of 1.55 μm . (b) Power spectrum calculated from the THz transient in (a).

axis of the black phosphorus is roughly aligned to the contacts of the antenna (within 20° offset).

The device was next characterized using a near-infrared gating wavelength of 1.55 μm . The gating beam was focused to a larger spot size in this experiment, leading to a lower gate fluence of 1.5 $\mu\text{J}/\text{cm}^2$. The THz transient and the corresponding spectrum are shown in Figure 5a,b, respectively. The pump power for the THz generation in this setup is about 1 order of magnitude smaller than the available power for the measurements at 800 nm, the signal current is also about 10 times smaller (cf. Figure 2a). Despite the significantly lower gating fluence, the measured current still reaches values of the same order of magnitude as at 800 nm, indicating that the device might benefit from operating at even lower photon energies. The highest SNR of about 30 dB is reached at a frequency of about 60 GHz and again drops to the noise level at above 0.2 THz. Because of the low pump power available in this setup, which limits the signal-to-noise ratio, we did not perform power or polarization dependence measurements. However, photocurrent measurements at this wavelength have shown similar behavior, indicating that the polarization and power dependence at 1.55 μm is similar that observed at 800 nm.

The utilization of black phosphorus as active material in photoconductive antennas for THz detection has two main advantages: Its low band gap extends the available wavelength range for gating to the mid-infrared range of up to 4 μm , and it can be combined with an arbitrary substrate material. While the growth of InGaAs devices via molecular beam epitaxy requires lattice matched substrates, for example, InP,⁹ flakes of black phosphorus can be transferred to arbitrary substrates. SiO₂ on Si is most commonly used for the fabrication of black phosphorus devices,¹⁴ but other substrates like SiC²⁴ or other two-dimensional (2D) materials are possible,²⁸ even the combination with optical waveguides is feasible.²⁹ Graphene also provides a high carrier mobility, necessary for photoconductive THz antennas, but so far only on-chip picosecond pulse generation and detection has been demonstrated.³⁰

The measured photocurrent I as a function of the time delay Δt between NIR and THz pulse can be approximated by

$$I(\Delta t) = e\mu\tau f \int_{-\infty}^{\infty} E(t)n(t - \Delta t)dt \quad (1)$$

where e is the electron charge, τ is the carrier lifetime, and f is the repetition rate of the laser.²⁵ The measured current is proportional to the carrier mobility μ , emphasizing the important role of the high mobility of about 900 V \cdot s/cm² achieved in our device. The electric field in the photoconductive channel is represented by $E(t)$ and is determined by

the incoming THz pulse and the antenna characteristics. In our case, the bow-tie antenna leads to a strong enhancement of the low frequency part of the spectrum.³¹ We estimate the resonance frequency of the antenna from the diameter of 1 mm and the effective refractive index, which is calculated from the refractive index of air (1) and Si (~ 3.5) to be 2.57. Assuming a half-wavelength dipole antenna, the predicted resonance frequency is 58 GHz, which matches the peak observed in our measurements well. In order for the measured current to directly resemble the THz waveform, the gating pulse induced carrier population $n(t)$ has to follow a delta function, or at least be a lot shorter than the duration of the THz pulse. However, the long carrier lifetime of black phosphorus does not exclude photoconductive THz detection:^{32,33} As long as the optical gating pulse (which is about 80 fs in our experiment) is short compared to the THz pulse duration, the carrier concentration can be approximated by a step function

$$n(t) = \begin{cases} 0, & t < 0 \\ n_0, & t \geq 0 \end{cases} \quad (2)$$

In this case, the measured current can be described by

$$I(\Delta t) = e\mu\tau f n_0 \int_{\Delta t}^{\infty} E(t)dt \quad (3)$$

which means that the derivative of the measured current follows the initial THz waveform. However, the integration process leads to a $1/\omega$ scaling of the measured spectrum that pronounces, like the antenna, the low-frequency part of the spectrum, which might be one reason for the low cutoff frequency of the device presented in our study. Pump-probe measurements on multilayer black phosphorus revealed a carrier lifetime of several hundreds of picoseconds.^{24,34} One route to increase the cutoff frequency of black phosphorus photoconductive THz detectors could be shortening the carrier lifetime by ion implantation which leads to faster recombination and scattering at defects. For example, the carrier lifetime in GaAs can be reduced by more than 2 orders of magnitude via carbon irradiation.³⁵ Decreasing the carrier lifetime would lead to a lower signal current but at the same time decreases the noise. Ideally, only the carrier lifetime would be reduced but not the mobility as the signal current scales in proportion to the latter. In this case, two effects lead to an improved signal-to-noise ratio: the higher dark resistivity would lower the Johnson current noise that is proportional to $1/R$, furthermore the noise of the photo current would be strongly suppressed. Tani et al. compared photoconductive THz detectors based on semi-insulating GaAs and low-temperature grown (LT) GaAs, which

revealed an improvement of more than 1 order of magnitude in the signal-to-noise ratio.³⁶ A part of the noise was attributed to the long-lived photoexcited carriers in the GaAs. Because the dark resistivity of our device is lower than in typical photoconductive antennas, we expect similar improvement in performance if the carrier lifetime could be reduced while maintaining the mobility. Furthermore, a higher dark resistivity would allow applying a high bias voltage and the possibility of utilizing black phosphorus as a photoconductive THz emitter. In addition, recent progress in the fabrication of large area films of black phosphorus creates the opportunity for developing large area photoconductive THz devices.^{37,38}

Another approach for device optimization would be the optimization of the device geometry. From the mobility μ and the channel length $l = 10 \mu\text{m}$ of our device and the peak electric field E of the THz pulse of about 3 V/cm we can derive the transit time τ_{tr} via³⁹ $\tau_{\text{tr}} = \frac{l}{2\mu E}$ to be around 200 ns. Note that this number strongly underestimates the driving electric field, as the antenna is not taken into account. From the geometrical ratio of the outer diameter of the antenna (1 mm) and the channel length (10 μm), we estimate an increase of the electric field in the channel by a factor of 100. We therefore expect the transit time to be around 2 ns, which is still significantly longer than the carrier lifetime. Decreasing the channel length potentially increases the cutoff frequency in two ways: it increases the electric field driving the carriers through the channel, while the shorter channel length directly decreases the transit time. By reducing the channel length to about 3 μm , the transit time is estimated to decrease by a factor of 10, leading to a transit time limited device with higher efficiency and cutoff frequency. Youngblood et al. demonstrated a reduction of the response time of a black phosphorus device to about 60 ps at bias fields of up to 6.7 kV/cm.³⁹ Such a short response time is about 1 order of magnitude below the carrier lifetime observed in our device.^{16,24} A recent study on photoconductive THz detection with semi-insulating GaAs, which like black phosphorus features a rather long carrier lifetime, demonstrates a 40-fold increase of the observed peak current and a significant increase of the cut off frequency by utilizing nanoscaled gaps between the electrodes.⁴⁰ Compared to these more conventional materials, for example, semi-insulating GaAs or low-temperature grown GaAs, the high dark conductivity of the black phosphorus leads to a higher noise. Whereas black phosphorus cannot compete directly with such materials, it is a versatile platform for specific applications requiring flexible substrates, substrates that are incompatible with commonly used semiconductors, or scenarios where a longer gating wavelength is used.

In conclusion, we present THz detection with a photoconductive antenna device based on black phosphorus. Polarization-resolved measurement revealed the role of the antenna that is most efficiently concentrating the electric field when the radiation is polarized along the bow-tie structure. THz transients recorded at gating wavelengths of 800 nm and 1.55 μm demonstrate the versatility of the device, which is expected to work out to 4 μm . The measured signal exhibits an approximately linear scaling with the applied THz field and with the square root of the applied near-infrared power. A maximum signal-to-noise ratio in the power spectrum of 40 dB is reached, which is sufficient for real spectroscopic applications. The measured spectrum peaks at 60 GHz and decreased for higher frequency until it reaches noise level at around 0.2 THz.

Narrowing the device channel would lead to a carrier transit time limited response that would both improve efficiency and increase the detection bandwidth.

AUTHOR INFORMATION

Corresponding Author

*E-mail: martin@mittendorff.email

ORCID

Martin Mittendorff: 0000-0003-3998-2518

Thomas E. Murphy: 0000-0002-8286-3832

Notes

The authors declare no competing financial interest.

ACKNOWLEDGMENTS

Parts of this work were supported by the Office of Naval Research (ONR) Award No. N000141310865 and the National Science Foundation (NSF) Award No. ECCS1309750. The sample fabrication was carried out at the University of Maryland Nanocenter.

REFERENCES

- (1) Auston, D. H.; Cheung, K. P.; Smith, P. R. Picosecond photoconducting Hertzian dipoles. *Appl. Phys. Lett.* **1984**, *45*, 284.
- (2) Grischkowsky, D.; Keiding, S.; van Exter, M.; Fattinger, Ch. Far-infrared time-domain spectroscopy with terahertz beams of dielectrics and semiconductors. *J. Opt. Soc. Am. B* **1990**, *7*, 2006–2015.
- (3) Frankel, M. Y.; Tadayon, B.; Carruthers, T. F. Integration of low temperature GaAs on Si substrates. *Appl. Phys. Lett.* **1993**, *62*, 255.
- (4) Jepsen, P. U.; Jacobsen, R. H.; Keiding, S. R. Generation and detection of terahertz pulses from biased semiconductor antennas. *J. Opt. Soc. Am. B* **1996**, *13*, 2424.
- (5) Takazato, A.; Kamakura, M.; Matsui, T.; Kitagawa, J.; Kadoya, Y. Terahertz wave emission and detection using photoconductive antennas made on low-temperature-grown InGaAs with 1.56 μm pulse excitation. *Appl. Phys. Lett.* **2007**, *91*, 011102.
- (6) Suzuki, M.; Tonouchi, M. Fe-implanted InGaAs terahertz emitters for 1.56 μm wavelength excitation. *Appl. Phys. Lett.* **2005**, *86*, 051104.
- (7) Chimot, N.; Mangeney, J.; Joulaud, L.; Crozat, P.; Bernas, H.; Blary, K.; Lampin, J. F. Terahertz radiation from heavy-ion-irradiated In_{0.53}Ga_{0.47}As photoconductive antenna excited at 1.55 μm . *Appl. Phys. Lett.* **2005**, *87*, 193510.
- (8) Sartorius, B.; Roehle, H.; Künzel, H.; Böttcher, J.; Schlak, M.; Stanze, D.; Venghaus, H.; Schell, M. All-fiber terahertz time-domain spectrometer operating at 1.5 μm telecom wavelengths. *Opt. Express* **2008**, *16*, 9565–9570.
- (9) Dietz, R. J. B.; Gerhard, M.; Stanze, D.; Koch, M.; Sartorius, B.; Schell, M. THz generation at 1.55 μm excitation: six-fold increase in THz conversion efficiency by separated photoconductive and trapping regions. *Opt. Express* **2011**, *19*, 25911–25917.
- (10) Mittendorff, M.; Xu, M.; Dietz, R. J. B.; Künzel, H.; Sartorius, B.; Schneider, H.; Helm, M.; Winnerl, S. Large area photoconductive terahertz emitter for 1.55 μm excitation based on an InGaAs heterostructure. *Nanotechnology* **2013**, *24*, 214007.
- (11) Preu, S.; Mittendorff, M.; Lu, H.; Weber, H. B.; Winnerl, S.; Gossard, A. C. 1550nm ErAs:In(Al)GaAs large area photoconductive emitters. *Appl. Phys. Lett.* **2012**, *101*, 101105.
- (12) Xu, M.; Mittendorff, M.; Dietz, R. J. B.; Künzel, H.; Sartorius, B.; Göbel, T.; Schneider, H.; Helm, M.; Winnerl, S. Terahertz generation and detection with InGaAs-based large-area photoconductive devices excited at 1.55 μm . *Appl. Phys. Lett.* **2013**, *103*, 251114.
- (13) Castellanos-Gomez, A.; Vicarelli, L.; Prada, E.; Island, J. O.; Narasimha-Acharya, K. L.; Blanter, S. I.; Groenendijk, D. J.; Buscema, M.; Steele, G. A.; Alvarez, J. V.; Zandbergen, H. W.; Palacios, J. J.; van der Zant, H. S. J. Isolation and characterization of few-layer black phosphorus. *2D Mater.* **2014**, *1*, 025001.

- (14) Xia, F.; Wang, H.; Jia, Y. Rediscovering black phosphorus as an anisotropic layered material for optoelectronics and electronics. *Nat. Commun.* **2014**, *5*, 4458.
- (15) Tran, V.; Soklaski, R.; Liang, Y.; Yang, L. Layer-controlled band gap and anisotropic excitons in few-layer black phosphorus. *Phys. Rev. B: Condens. Matter Mater. Phys.* **2014**, *89*, 235319.
- (16) Suess, R. J.; Leong, E.; Garrett, J. L.; Zhou, T.; Salem, R.; Munday, J. N.; Murphy, T. E.; Mittendorff, M. Midinfrared time-resolved photoconduction in black phosphorus. *2D Mater.* **2016**, *3*, 041006.
- (17) Viti, L.; Hu, J.; Coquillat, D.; Knap, W.; Tredicucci, A.; Politano, A.; Vitiello, M. S. Black phosphorus terahertz photodetectors. *Adv. Mater.* **2015**, *27*, 5567–5572.
- (18) Viti, L.; Hu, J.; Coquillat, D.; Politano, A.; Knap, W.; Vitiello, M. S. Efficient Terahertz detection in blackphosphorus nano-transistors with selective and controllable plasma-wave, bolometric and thermoelectric response. *Sci. Rep.* **2016**, *6*, 20474.
- (19) Wang, L.; Liu, C.; Chen, X.; Zhou, J.; Hu, W.; Wang, X.; Li, J.; Tang, W.; Yu, A.; Wang, S.-W.; Lu, W. Toward sensitive room-temperature broadband detection from infrared to terahertz with antenna-integrated black phosphorus photoconductor. *Adv. Funct. Mater.* **2017**, *27*, 1604414.
- (20) Leong, E.; Suess, R. J.; Sushkov, A. B.; Drew, H. D.; Murphy, T. E.; Mittendorff, M. Terahertz photoresponse of black phosphorus. *Opt. Express* **2017**, *25*, 12666–12674.
- (21) Kim, J.-S.; Liu, Y.; Zhu, W.; Kim, S.; Wu, D.; Tao, L.; Dodabalapur, A.; Lai, K.; Akinwande, D. Toward air-stable multilayer phosphorene thin-films and transistors. *Sci. Rep.* **2015**, *5*, 8989.
- (22) Dreyhaupt, A.; Winnerl, S.; Dekorsy, T.; Helm, M. High-intensity terahertz radiation from a microstructured large-area photoconductor. *Appl. Phys. Lett.* **2005**, *86*, 121114.
- (23) Janke, C.; Först, M.; Nagel, M.; Kurz, H.; Bartels, A. Asynchronous optical sampling for high-speed characterization of integrated resonant terahertz sensors. *Opt. Lett.* **2005**, *30*, 1405–1407.
- (24) Suess, R. J.; Jadidi, M. M.; Murphy, T. E.; Mittendorff, M. Carrier dynamics and transient photobleaching in thin layers of black phosphorus. *Appl. Phys. Lett.* **2015**, *107*, 081103.
- (25) Tani, M.; Sakai, K.; Mimura, H. Ultrafast Photoconductive Detectors Based on Semi-Insulating GaAs and InP. *Jpn. J. Appl. Phys.* **1997**, *36*, L1175–1178.
- (26) Zhang, G.; Huang, S.; Chaves, A.; Song, C.; Özçelik, V. O.; Low, T.; Yan, H. Infrared fingerprints of few-layer black phosphorus. *Nat. Commun.* **2017**, *8*, 14071.
- (27) Guo, Q.; Pospischil, A.; Bhuiyan, M.; Jiang, H.; Tian, H.; Farmer, D.; Deng, B.; Li, C.; Han, S.-J.; Wang, H.; Xia, Q.; Ma, T.-P.; Mueller, T.; Xia, F. Black Phosphorus Mid-Infrared Photodetectors with High Gain. *Nano Lett.* **2016**, *16*, 4648–4655.
- (28) Chen, X.; Wu, Y.; Wu, Z.; Han, Y.; Xu, S.; Wang, L.; Ye, W.; Han, T.; He, Y.; Cai, Y.; Wang, N. High-quality sandwiched black phosphorus heterostructure and its quantum oscillations. *Nat. Commun.* **2015**, *6*, 7315.
- (29) Youngblood, N.; Chen, C.; Koester, S. J.; Li, M. Waveguide-integrated black phosphorus photodetector with high responsivity and low dark current. *Nat. Photonics* **2015**, *9*, 247–252.
- (30) Hunter, N.; Mayorov, A. S.; Wood, C. D.; Russell, C.; Li, L.; Linfield, E. H.; Davies, A. G.; Cunningham, J. E. On-Chip Picosecond Pulse Detection and Generation Using Graphene Photoconductive Switches. *Nano Lett.* **2015**, *15*, 1591–1596.
- (31) Tani, M.; Matsuura, S.; Sakai, K.; Nakashima, S.-i. Emission characteristics of photoconductive antennas based on low-temperature-grown GaAs and semi-insulating GaAs. *Appl. Opt.* **1997**, *36*, 7853–7859.
- (32) Sun, F. G.; Wagoner, G. A.; Zhang, X.-C. Measurement of free-space terahertz pulses via long-lifetime photoconductors. *Appl. Phys. Lett.* **1995**, *67*, 1656.
- (33) Castro-Camus, E.; Fu, L.; Lloyd-Hughes, J.; Tan, H. H.; Jagadish, C.; Johnston, M. B. Photoconductive response correction for detectors of terahertz radiation. *J. Appl. Phys.* **2008**, *104*, 053113.
- (34) Ge, S.; Li, C.; Zhang, Z.; Zhang, C.; Zhang, Y.; Qiu, J.; Wang, Q.; Liu, J.; Jia, S.; Feng, J.; Sun, D. Dynamical Evolution of Anisotropic Response in Black Phosphorus under Ultrafast Photoexcitation. *Nano Lett.* **2015**, *15*, 4650–4656.
- (35) Deshmukh, P.; Mendez-Aller, M.; Singh, A.; Pal, S.; Prabhu, S. S.; Nanal, V.; Pillay, R. G.; Döhler, G. H.; Preu, S. Continuous wave terahertz radiation from antennas fabricated on C12-irradiated semi-insulating GaAs. *Opt. Lett.* **2015**, *40*, 4540–4543.
- (36) Liu, T.-A.; Tani, T.-A. L.; Nakajima, M.; Pan, M. H.-L. Ultrabroadband terahertz field detection by photoconductive antennas based on multi-energy arsenic-ion-implanted GaAs and semi-insulating GaAs. *Appl. Phys. Lett.* **2003**, *83*, 1322.
- (37) Smith, J. B.; Hagaman, D.; Ji, H.-F. Growth of 2D black phosphorus film from chemical vapor deposition. *Nanotechnology* **2016**, *27*, 215602.
- (38) Kaur, H.; Yadav, S.; Srivastava, A. K.; Singh, N.; Schneider, J. J.; Sinha, Om. P.; Agrawal, V. V.; Srivastava, R. Large Area Fabrication of Semiconducting Phosphorene by Langmuir-Blodgett Assembly. *Sci. Rep.* **2016**, *6*, 34095.
- (39) Youngblood, N.; Li, M. Ultrafast photocurrent measurements of a black phosphorus photodetector. *Appl. Phys. Lett.* **2017**, *110*, 051102.
- (40) Heshmat, B.; Pahlevaninezhad, H.; Pang, Y.; Masnadi-Shirazi, M.; Lewis, R. B.; Tiedje, T.; Gordon, R.; Darcie, T. E. Nanoplasmonic Terahertz Photoconductive Switch on GaAs. *Nano Lett.* **2012**, *12*, 6255–6259.